PATH LOSS MEASUREMENTS AND MODEL ANALYSIS OF A 2.4 GHZ WIRELESS NETWORK IN AN OUTDOOR ENVIRONMENT

A Thesis
Presented to
The Academic Faculty

By

Lorne C. Liechty

In Partial Fulfillment
Of the Requirements for the Degree
Master of Science in Electrical Engineering

Georgia Institute of Technology

August, 2007

PATH LOSS MEASUREMENTS AND MODEL ANALYSIS OF A 2.4 GHZ NETWORK IN AN OUTDOOR ENVIRONMENT

Approved By:

Gregory D. Durgin
School of Electrical and Computer Engineering
Georgia Institute of Technology

Andrew F. Peterson
School of Electrical and Computer Engineering
Georgia Institute of Technology

Robert J. Butera
School of Electrical and Computer Engineering
Georgia Institute of Technology

Date Approved: May 07, 2007

To my parents

ACKNOWLEDGEMENTS

Firstly, before anything else, I'd like to thank Jesus Christ. This degree, my job, my wife, my family… they were all His ideas. My greatest hope is that He will be pleased with all that I have done with what He gave me.

Next, I'd like to thank my wife Maryanne. I love her more every day, and even though we're still just starting what will hopefully be a long road together, being with her it feels like we've been friends forever. Thank you for being my support every day of the week. (Also, thanks for watching baby Hannah all day while I'm gone doing research! I like to come home and just be the "fun parent".)

I've already dedicated this work to my parents, but I feel that they deserve extra thanks for taking me all the way to the doorstep of reality before I took my first steps into the "grown-up" world. All of my work ethic and determination comes from seeing both my parents push themselves towards excellence all my life.

Greg Durgin has been an incredible advisor so far in my graduate career. He is ever the cheerleader for his students and a true master at helping fragile ideas blossom into great research. I hope to someday be an equally energetic and caring advisor for students of my own.

Now to thank all my friends at Motorola! First, I have to say thanks to the whole RF Design and Management software development team for expecting a lot from me and welcoming my ideas (even the bad ones). Thanks to Veera Anantha for putting forth the extra effort to keep me employed and working on fun projects. Thanks to Eric Reifsnider for giving me guidance and direction all through my various research projects. Thanks to

Keith Astoria for destroying all my prior knowledge of programming and teaching me how to do it properly. And just so that I don't leave anyone off; thanks to Keith Bray, Matt Zappitello, Kevin Albert, Steve Williams, Gemei Yang, Eric Pope, Bobby Basak, Mohammad Minhas, Roger Skidmore, and Mike Watts.

Lastly, I have to say thanks to all the great people in the Propagation Group at Georgia Tech. Thanks to Ryan Pirkl, Josh Griffin, Chris Durkin, Albert Lu, Cody Lamb, Rikai Huang, and Alex Trzecieski, you guys are one of the smartest collections of people I've ever been around. Who knew research could be so entertaining?

TABLE OF CONTENTS

LIST OF TABLES

LIST OF FIGURES

SUMMARY

Careful network planning has become increasingly critical with the rising deployment, coverage, and congestion of wireless local area networks (WLANs). This thesis outlines the achieved prediction accuracy of a direct-ray, single path loss exponent, adapted Seidel-Rappaport propagation model as determined through measurements and analysis of the established 2.4 GHz, 802.11g outdoor WiFi network deployed on the campus of the Georgia Institute of Technology. Additionally, the viability of using the obtained model parameters as a means for planning future network deployment is discussed. Analysis of measured data shows that accurate predictive planning for network coverage is possible without the need for overly complicated modeling techniques such as ray tracing. The proposed model performs with accuracy comparable to other commonly accepted, more complicated models and is offered as a simple, yet strong predictive model for network planning – having both speed and accuracy. Results show, that for the area under study, the standard deviation of the prediction error for the proposed model is below 6.8dB in all analyzed environments, and is approximately 5.5dB on average. Further, the accuracy of model predictions in new environments is shown to be satisfactory for network planning.

CHAPTER 1:
INTRODUCTION

With the worldwide proliferation and subsequent congestion of wireless local area networks (WLANs), careful network planning and propagation modeling have become essential to current deployments. In the past, early outdoor WiFi coverage has been estimated in largely an ad hoc manner: infrastructure was placed in a small test area with a basic idea of coverage in mind, using measurement surveys to provide verification and analysis, and then repeating the process for more and more areas until full coverage is achieved. This process can be very costly and time-consuming.

An alternative approach that promises lowered cost and lowered time-to-deployment is the Adaptive Deployment method, proposed in this report. The Adaptive Deployment method consists of a site-survey and analysis processes on an initial test area and then use of the analysis of this test area to update parameters for a predictive model, which can then be used to simulate the deployment process in other areas. Using the optimized predictive model, a network planner can determine the placement and amount of infrastructure required to meet the demands of the network for a deployment of any size. By planning the full deployment using this Adaptive Deployment design methodology, the number of cyclic deploy-and-verify steps can be drastically reduced.

In order to exercise predictive deployment in this fashion, the network calculations must use a path loss model that is both accurate and capable of being optimized. To accomplish this, an adaptation of the Seidel-Rappaport propagation model [5] is used as a simple, accurate direct-ray, single path loss exponent, model which can be

used for predictions in the outdoor environment. The Seidel-Rappaport model is capable of being optimized using standard linear regression techniques [11], and has significant speed advantages compared to more complicated models, such as ray-tracing. Further, the model allows for the inclusion of site-specific environment information to improve accuracy as compared to a purely distance dependent, free-space path loss model.

The measurements and analysis in this paper demonstrate the validity of the Adaptive Deployment design methodology and the use of a direct-ray, single path loss exponent, adapted Seidel-Rappaport path loss model in the outdoor space by analyzing the established 802.11g WiFi network on the campus of the Georgia Institute of Technology. From the results of the analysis, it is shown that the prediction error of the model under study is below 6.8dB for all analyzed environments and is approximately 5.5dB on average, which agrees well with other published path loss models for the outdoor domain. Further, the Adaptive Deployment process is validated since the average mean error offset for predictions into new environments at all data points is only -0.9dB and average standard deviation is approximately 7.0dB.

CHAPTER 2:
EXISTING OUTDOOR MODELING TECHNIQUES

Methods for predicting outdoor wireless signal coverage have been under development for decades. These models predict the signal power at a given point by determining the path loss, the difference between the transmit power and received power, from the transmitter to the receiver. Deterministic propagation models generally fall into two categories: Direct-Ray and Multi-Ray models.

2.1: Direct-Ray Models

Direct-Ray models, as described in this paper, are those that calculate the signal path loss based on parameters determined from the shortest straight line connecting the transmitting and receiving antennas. The simplest of these models is the purely distance dependent Friis transmission equation, which calculates the received signal power according to the signal loss in free space using:

$$P_{Rx} = P_{Tx} \cdot G_{Tx} \cdot G_{Rx} \cdot \left(\frac{\lambda}{4\pi \cdot d} \right)^2 \qquad 1$$

where P_{Rx} is the signal power at the receiver, P_{Tx} is the signal power output from the transmitter, G_{Tx} is the gain of the transmitting antenna, G_{Rx} is the gain of the receiving antenna, λ is the wavelength, and d is the distance from the transmitter to the receiver. The Friis transmission equation makes the assumption that the propagation environment is essentially vacuous, which limits its applicability in real world environments.

In order to increase the accuracy of the Friis transmission equation, the exponential term is raised to the general power n, which is referred to as the path loss

exponent, in a vacuum n is equal to 2. The path loss exponent allows site-specific variations to be included in the distance dependent model and is one of the most important parameters of all distance dependent models. With the inclusion of the path loss exponent, the standard path loss equation takes the form:

$$PathLoss = 10 \cdot n \cdot \log_{10}\left(\frac{d}{d_0}\right) + 20 \cdot \log_{10}\left(\frac{4\pi \cdot d_0}{\lambda}\right) + \mathrm{X}_{\sigma} \qquad 2$$

where the included parameters are the previously mentioned path loss exponent, n, a reference distance d_0, and the term X_σ, which represents accepted log-normal variation in the channel path loss. This form of the equation isolates the loss components of the Friis transmission equation by grouping the difference of the received power to the transmitter power and antenna gains into a single path loss term. The equation is almost exclusively manipulated in logarithmic scale.

Some direct-ray models will use multiple path loss exponents depending on the RF environment encountered by the direct-ray path, such as Line of Sight (LOS) where there are no obstructions between the transmitter and receiver and Non Line of Sight (NLOS) where there are obstructions between the transmitter and receiver. In other models two path loss exponents are used for the same LOS path as set by a geometry determined breakpoint distance [2] [3] [4].

Increased sophistication in Direct-Ray models generally involves the inclusion of additional parameters to the path loss equation given in 2, for site-specific information which is correlated to signal gain or loss with respect to the free space loss. These parameters often include information regarding building heights [18] [19] [17], street width [19], building spacing [19] [17], and other physical information correlated to

known propagation mechanisms. While some parameters of Direct-Ray methods may be determined from knowledge of multipath (or multiple ray) components, the models still do not involve direct calculations of multiple ray paths.

2.2: Multi-Ray Models

Multi-Ray methods, as described in this paper, are those that calculate the signal path loss based on the aggregation of the field strength for more than one path from the transmitter to the receiver. Typically Multi-Ray models are described under the umbrella of ray-tracing models, but the term Multi-Ray is used herein to include any model which may aggregate the signal strength contribution of more than one transmitter-to-receiver path at a time.

Multi-Ray models usually make direct calculations of path loss based on paths determined by geometric reflections, diffractions, and scattering [1], rather than making more indirect calculations of path loss due to correlations as in Direct-Ray methods. Many full ray tracing methods focus on launching a large number of rays from the transmitter to the receiver and use geometric optics to determine the subsequent paths of the rays [1]. Other methods focus on selecting only those ray paths which make the largest contributions to the received signal power [14] [15] [16]. The additional complexity of Multi-Ray models brings vastly increased computation time as compared to Direct-Ray models, and this has made them difficult to use in large-scale network planning.

CHAPTER 3:
MEASUREMENT METHODOLOGY

3.1: Hardware

In this study a NETGEAR™ WAG 511 v2 WLAN card (shown in Figure 1) is used as the measurement receiver. This card is controlled with special Motorola drivers and Motorola MeshPlanner™ software installed on the client laptop which permits collection of so-called RF Monitoring mode measurements. In this mode, the card is prohibited from making an association to any access point (AP), but instead scans all WiFi channels of interest and then makes measurements of the Received Signal Strength Indication (RSSI) for each AP it samples. Using this method, it is possible to measure all APs whose RSSI is within the dynamic range of the card at any given point.

Figure 1: The NETGEAR™ WLAN card used as the receiver device in all surveys

The receiver sensitivity is very important in any wireless measurement survey. If the receiver sensitivity is poor, important measurements at the bottom end of the power range may be excluded from the measurement survey, and subsequently may skew the analysis of the data. The sensitivity of the WLAN card used in this survey is stated to be -94dBm by the manufacturer's specifications.

The WLAN card used for the survey utilized an internal antenna. The exact antenna pattern is unknown; however, it can be safely assumed that the antenna can be approximated by an isotropic pattern due to its electrically small design and the unpredictability of the slight effects which may be induced by near-field coupling to the accompanying laptop. All WLAN cards with integrated antennas will tend to have these similar features. Further, test measurements made at various orientations indicate that the antenna has low directivity, and therefore a 0dBi, isotropic pattern is assumed.

Overall, the effect of using a WLAN card for measurement of a wireless network will have little effect on the analysis of network performance or analysis of the performance of the predictive propagation model. That is, so long as it is understood that any analysis will have been inherently calibrated to the WLAN card receiver being used in the survey. Obviously, using a receiver with increased sensitivity will likely have some effect on the analysis by including more points into the dataset under analysis. Further, individual WLAN cards may be calibrated or designed differently and are well known to produce slightly different results between cards for the measured RSSI at a given points, but this difference was found to be within 1 to 2 dB on average and therefore not a significant source of error.

3.2: Data Collection Procedure

Beyond hardware used in the measurement campaign, the method by which measurements are taken can have a significant impact on the reliability of the data obtained. Sampling rate, velocity, spatial averaging, and other considerations need to be accounted for in the analysis of the measurements.

For the measurement surveys, the WLAN card was inserted into the PCMCIA slot on the side of a standard laptop. Throughout the surveys, the top of the card was oriented toward the zenith sky in order to best approximate typical device use by an end user of the network and to increase the likelihood that the direct-ray signal path falls within the half-power beamwidth of the antenna. This measurement orientation is shown in Figure 2.

Figure 2: When taking measurements, the laptop was kept in the orientation shown, with the top of the WLAN card pointed toward the zenith sky. This was done to maintain received pattern consistency throughout the survey.

In this study, two separate modes of measurement positioning were used: track run measurements and single marker measurements. Both methods require the locations of the measurements to be selected by the user through identification of the measurement location on a bird's-eye map of the general region. In the single marker measurement mode, the measured values are referenced to the user selected location, as determined by a mouse-click on the map of the area under measurement. For track run measurements, the user indicates a start and an end location, and the amount of time in between the input of those two points determines where each measurement in the run should be referenced along the straight line path from the start point to the end point.

In order to ensure that the track run measurements collected during this survey are not adversely affected by sampling delay, the measurements are all taken while walking at a relatively slow pace. Since the longest total sampling period used in the study was only six seconds, it is unlikely that there would be any effect due to sampling delay since the dimensions of the large scale fading effects in the outdoor space are all likely to be much larger than the distance traveled between measurement locations. Further, tests taken at a high sampling rate (greater than 1 sample/sec) and those taken at a low rate (less than 0.2 sample/sec) over the same region at the same walking speed showed similar standard deviation, mean error, and model parameter values after regression analysis. As such, the vast majority of measurements were taken using track-run mode since the largely quantity of measurement acquired will reduce susceptibility to small-scale fading in the channel.

If the distribution of measurements is not evenly spread across the full variety of the RF environment, then the results of the data analysis will end up favoring predictions

for one particular environment over another. This result will cause a spatial inconsistency in the accuracy of the model predictions. Therefore it is important not to have a significantly larger number of measurements in one particular area over another. In this study a hard limit was not defined for this aspect of the measurement survey, but the general practice was to avoid having an order-of-magnitude difference in the spatial distribution of the included measurements for a given region.

To provide additional illustration of the measurement procedure, Figure 3 and Figure 4 show some sample measurements in progress.

Figure 3: Lorne Liechty takes track run measurements of the Van Leer AP while walking slowly.

Figure 4: Lorne Liechty takes a single marker measurement of the Van Leer AP.

3.3: Scope of Measurement Survey

The scope of this analysis is limited to the campus of the Georgia Institute of Technology. While this campus is located in the Midtown area of Atlanta, the majority of the campus has significantly more green-space than the average urban (city) area. The APs used for analysis in this study are herein referenced with respect to which campus building they were mounted on, namely the Van Leer AP, the Zeta Tau Alpha Sorority House (ZTA) AP, and the Technology Square Research Building (TSRB) North and South APs. These APs were chosen based upon the availability of information regarding their hardware link configuration and antenna gain pattern. The APs used in the survey are illustrated in Figure 5 through Figure 8.

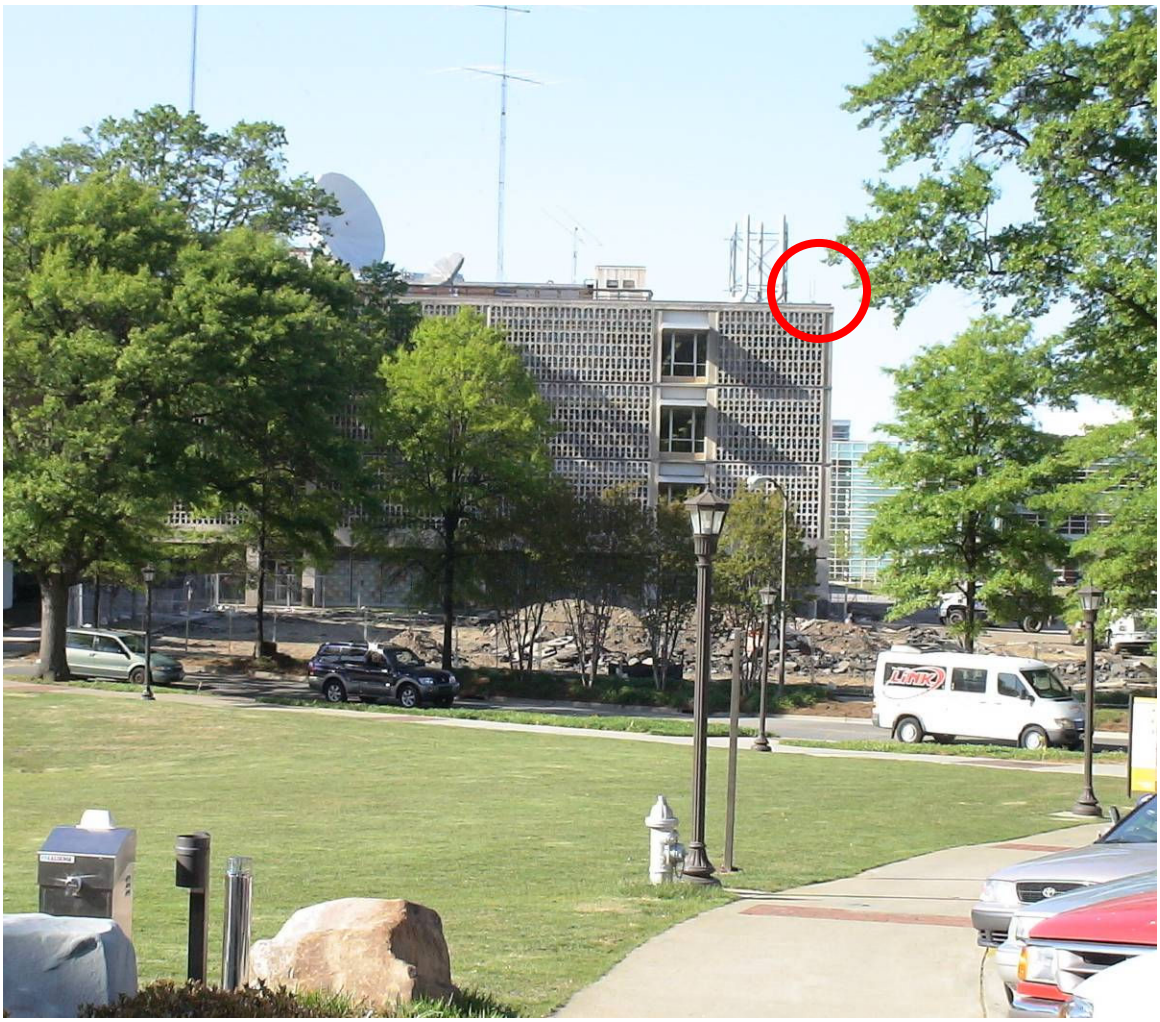

Figure 5: The Van Leer AP and surrounding area. The red circle indicates the location of the transmitting antenna.

Figure 6: The Zeta Tau Alpha (ZTA) AP and surrounding area. The red circle indicates the location of the transmitting antenna.

Figure 7: The Technology Square Research Building (TSRB) South AP and surrounding area. The red circle indicates the location of the transmitting antenna.

Figure 8: The Technology Square Research Building (TSRB) North AP and surrounding area. The red circle indicates the location of the transmitting antenna.

CHAPTER 4:
ENVIRONMENT MODELING METHODOLOGY

4.1: Geophysical Modeling

In the model under study, the local terrain, buildings, and foliage are included as the dominant factors in the path loss calculation. As such, models for each of these are included in the analysis. Fortunately, these types of datum are either freely available or easily obtained at cost for all of the United States and large portions of the rest of the world. For this study, terrain information was obtained at 10 meter resolution from the USGS public servers, building outlines and foliage boundaries for the campus were obtained from the Georgia Institute of Technology College of Architecture. For the purpose of the model, all building heights are set at 15.24m (an estimate of the average building height) and all foliage boundaries are set to a height of 6.10m (an estimate of the average tree height). A picture of the modeled campus with included building footprints, foliage, and terrain is shown in Figure 9 and Figure 10. The building and foliage data used for this analysis is the most up-to-date information that was readily available. Minor variations exist between the data included and the current environment, however, these are not considered to be detrimental to the analysis performed.

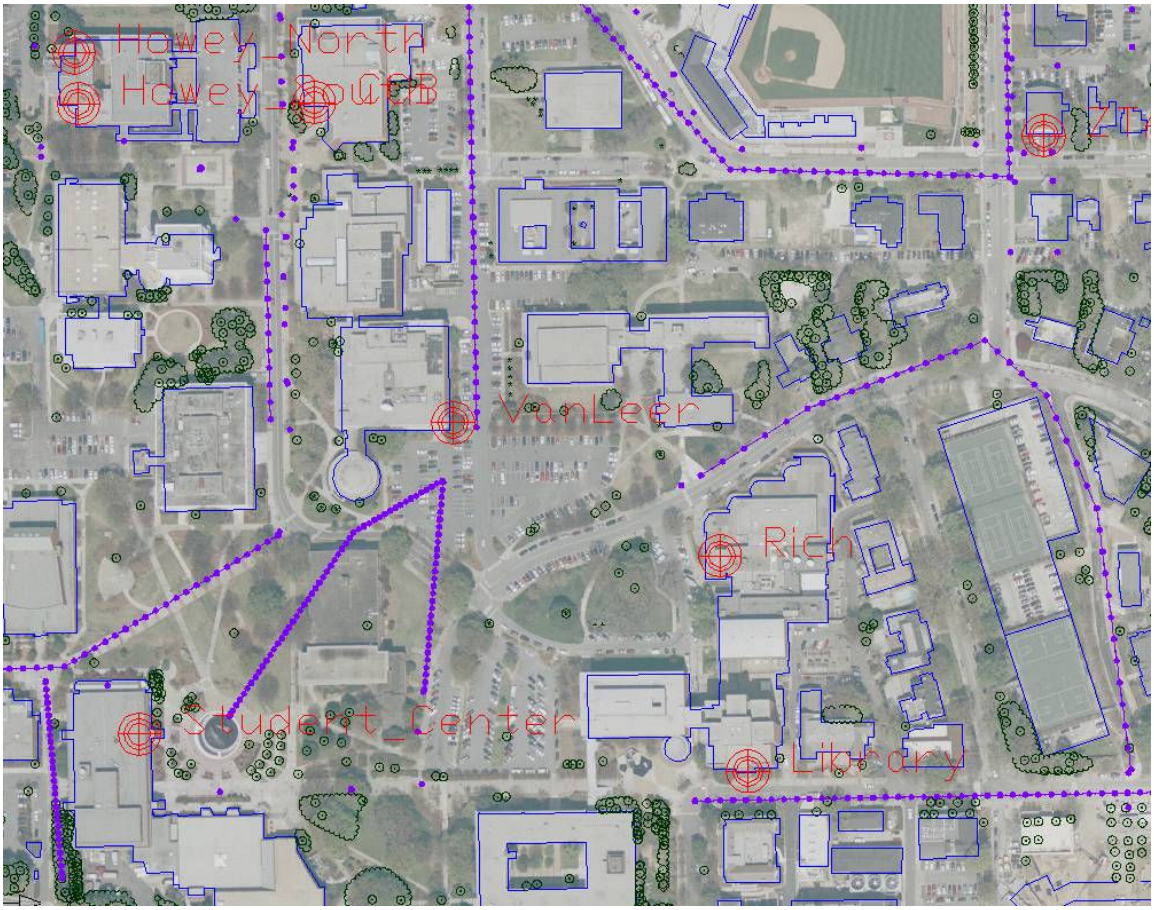

Figure 9: Diagram of a 0.48km x 0.59km area of the modeled campus environment obtained from a screen-capture of the Motorola MeshPlanner™ software. Building outlines and foliage boundaries are included as dominant path loss parameters in the model. Access points are placed above the terrain at empirically determined heights.

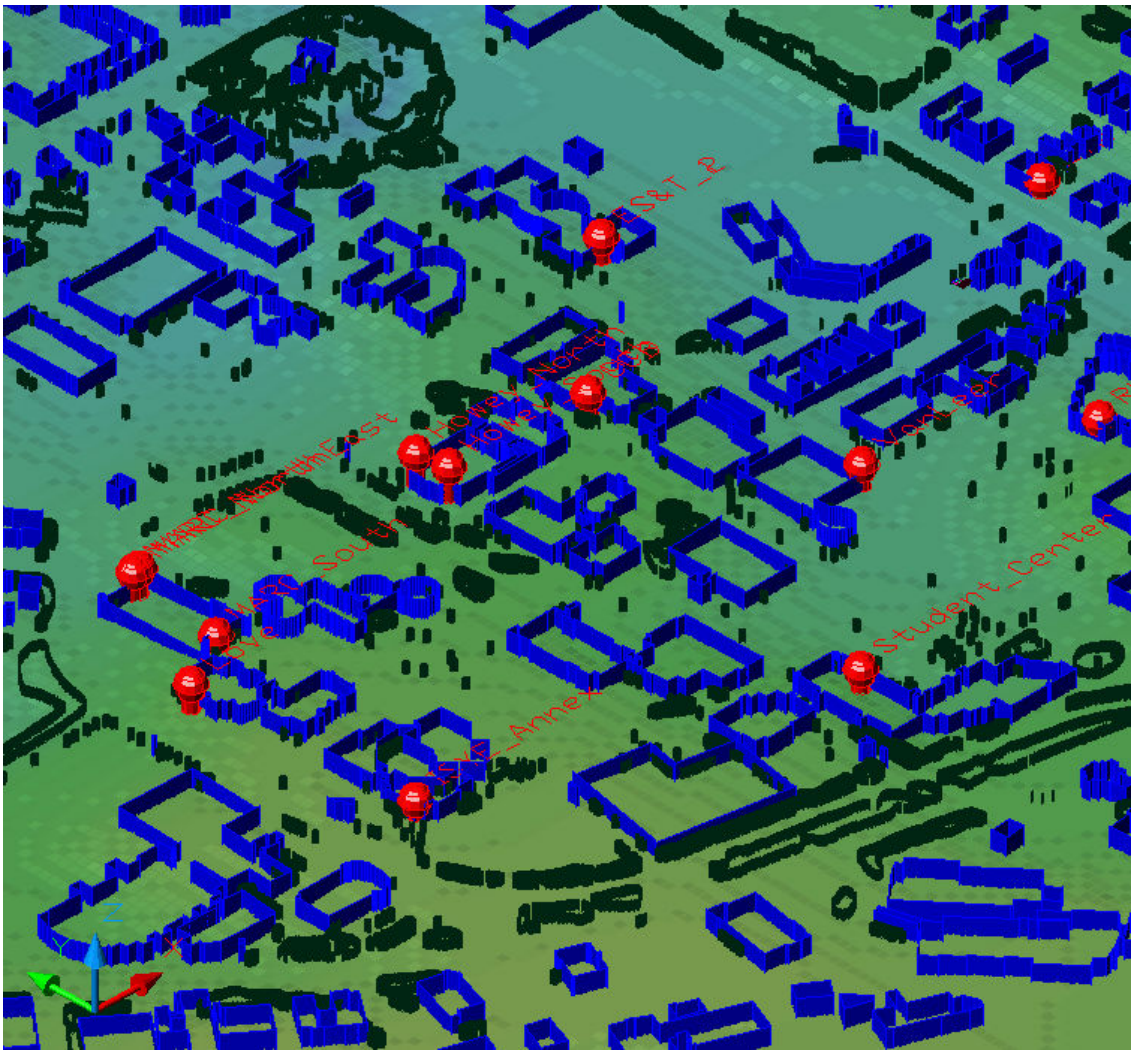

Figure 10: Three-dimensional, southwest isometric view of the modeled campus environment obtained from a screen-capture of the Motorola MeshPlanner™ software.

4.2: Modeling Installed WLAN Infrastructure

Beyond modeling just the surrounding RF environment, the WLAN infrastructure is modeled in order to perform accurate analysis of the path loss model. In this study, the established outdoor network at the campus of the Georgia Institute of Technology (the Local Area Walkup & Wireless Network or LAWN) is modeled and measured. With help from the University's Office of Information Technology, the locations, transmitter powers, and antenna gain patterns were obtained for a number of their outdoor transmit locations.

Additionally, the relative height to the local terrain and orientation of each antenna is necessary. The relative heights were estimated by measuring a fixed distance from the antenna mounting location and then using simple angle measurements and trigonometry to determine the height of the antenna. This method was checked for a building of known height and was found to be accurate to within two percent. The azimuth and elevation angles of orientation for the antennas were estimated by visual inspection.

In order to determine the path loss from the transmitter to the receiver, the output power of the transmitting antenna must be known. The output power of the AP was determined by referencing the current device settings of the hardware. The input power to the antenna was estimated either by using prior knowledge of the forward link from the AP to the antenna, or by visual inspection of the forward link equipment. After recording the quantity of connectors, cable, and amplifiers used in the construction of the forward link, the transmit power was estimated based on the manufacturer's specified values for signal loss or gain at each component.

In order to verify the described estimates of the antenna model, the output power of the Van Leer Antenna was measured using a power meter with a sufficiently large dynamic range, -70dBm to +44dBm, and an attached probe antenna, as shown in Figure 11. The power measurements of the antenna were determined to be satisfactory, within 1 to 2 dB of the estimated power for several sample measurement locations within the main beam of the antenna gain pattern.

Figure 11: One-meter test measurement process to verify estimates of the transmitter output power of the Van Leer AP.

For those antennas being analyzed in this study, the model number and manufacturer were recorded and used to determine the antenna gain pattern. Once the information for the elevation gain pattern and the azimuth gain pattern are obtained, the

value of the antenna gain at any given point can be determined by an elliptical interpolation between the azimuth and elevation values for the given angle [12].

In some cases, the exact pattern provided by the manufacturer contained very detailed pattern information with peaks and nulls that varied by only a few dB. Since this level of detail is not likely to remain accurate after installation of the antenna due to manufacturing variability, multipath effects, mounting configuration, and near-field coupling which may all distort the pattern, a smoothed antenna pattern was used to simplify the modeling procedure and still maintain an acceptable level of accuracy. Since the antennas used in the network were sectoral with wide half-power beamwidths, the smoothed pattern was derived from a cardioid using the following equations:

$$Gain(\theta) = (\cos\theta - 1) \cdot \frac{3}{\left(1 - \cos\left(\frac{HBW_\theta}{2}\right)\right)} \quad 3$$

$$Gain(\varphi) = (\cos\varphi - 1) \cdot \frac{3}{\left(1 - \cos\left(\frac{HBW_\varphi}{2}\right)\right)} \quad 4$$

Where θ is the azimuth bearing angle, φ is the elevation bearing angle, HBW_θ is the half-power beamwidth in the azimuth plane, and HBW_φ is the half-power beamwidth in the elevation plane. These equations calculate the approximate antenna pattern in logarithmic scale, and are one set of equations used for approximating directional antenna patterns within industry standard modeling software, Motorola Meshplanner™. A further approximation of the antenna pattern was made by thresholding the antenna pattern to a minimum gain value of 0dBi. Figure 12 and Figure 13 show an example of a manufacturer's gain pattern and the resulting gain pattern used in the model.

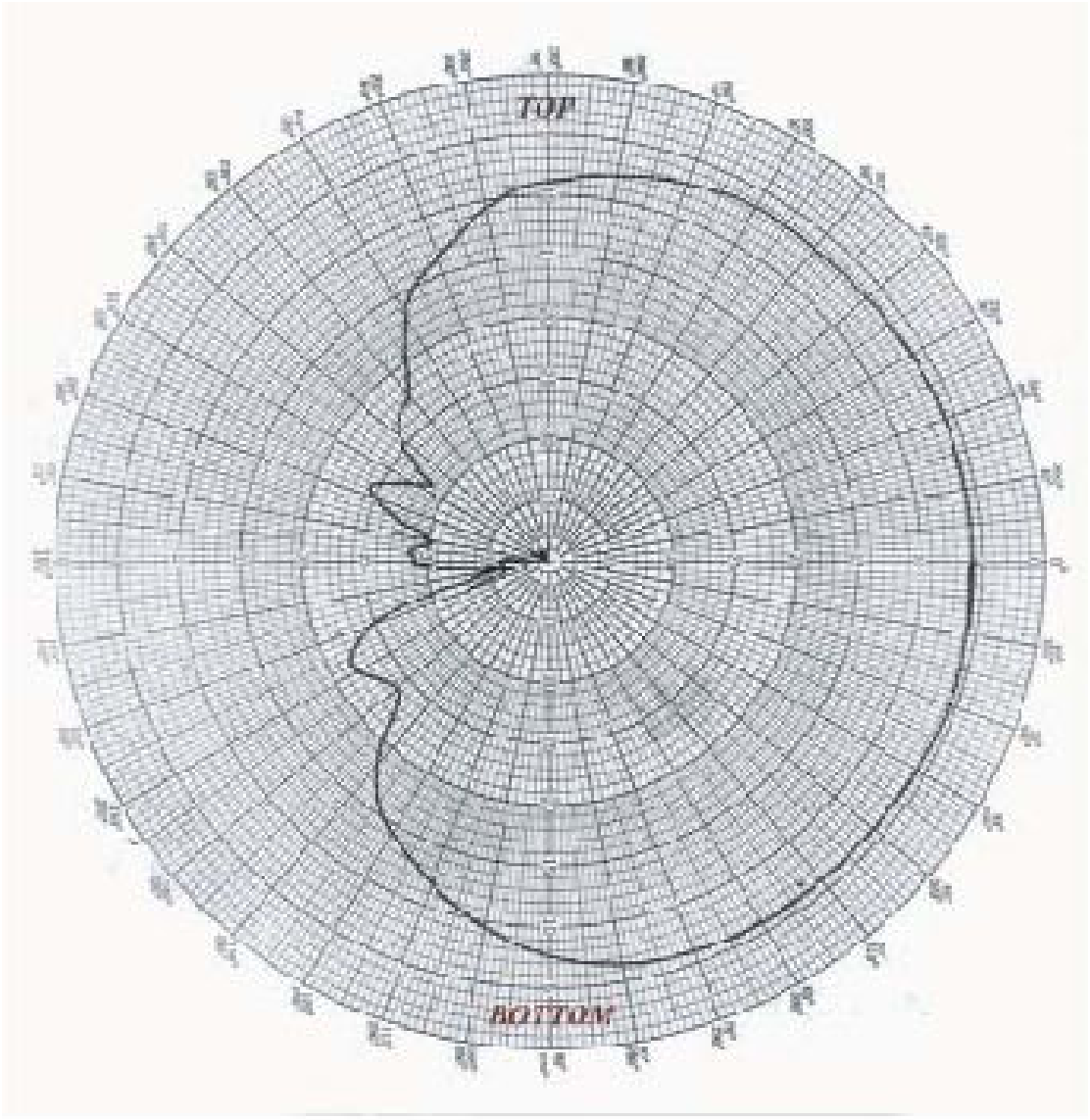

Figure 12: Antenna pattern for a 14.2dBi YDI sectoral antenna with a 180 degree half-power beamwidth.

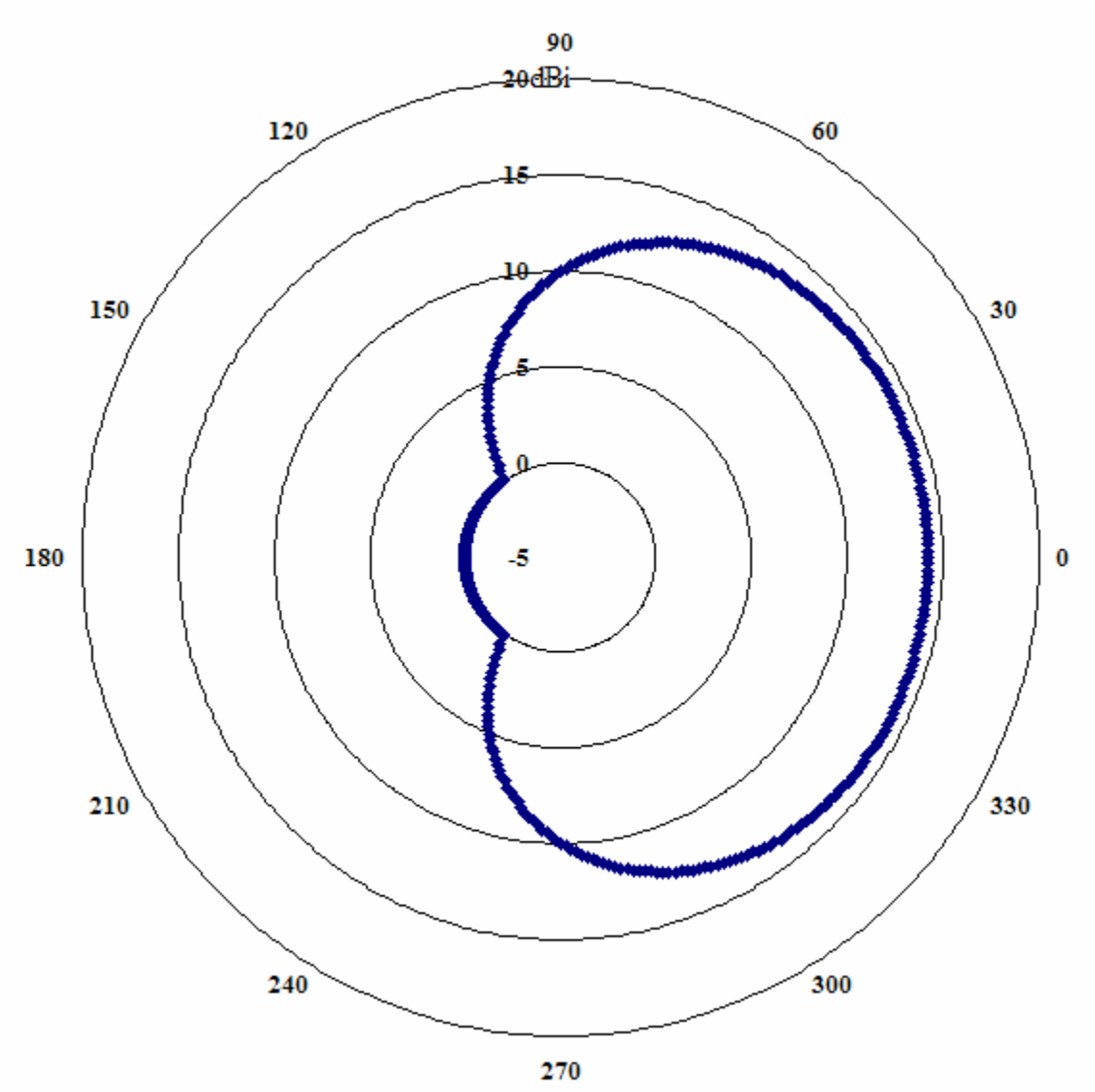

Figure 13: Example of antenna gain pattern smoothing used in environment model, pattern scale is in units of dBi. This pattern is the approximation of the 2.4GHz azimuth pattern used for a 14.2dBi YDI sectoral antenna with a 180 degree half-power beamwidth.

CHAPTER 5:
ANALYSIS OF MEASURED DATA

5.1: Description of the Model Under Study

The model used for this analysis is a direct-ray, single path loss exponent model developed at Motorola, Inc. This model is an outdoor, microcell adaptation of the Seidel-Rappaport model [5], which calculates the path loss based upon the transmitter-receiver separation distance and the number and type of obstructions intersecting the straight-line between the transmitter and receiver (direct-ray) [1]. In this analysis, intersections of the direct-ray signal path with building footprints (outlines) and foliage boundaries are included as the propagation affecting variables of the modeled environment. The equation for the signal path loss (in dB) used in this analysis is then given as:

$$PathLoss = PL(d_0) + 10n\log_{10}\left(\frac{d}{d_0}\right) + \sum_i OBS_i \cdot PE_i \qquad 5$$

where $PL(d_0)$ is equal to the free space path loss with respect to a given reference distance, d_0, (typically 1m, 100m, or 1km depending on the environment [6]), d is the distance between the transmitter and receiver, n is the path loss exponent, OBS_i is the number of obstructions of type i that intersect the direct-ray path from the transmitter to the receiver, and PE_i is the propagation effect, or amount of change in the path loss incurred per intersecting obstruction, for an obstruction of type i. In this study, d_0 is set to 1m.

As an example of how the path loss for this model is calculated, consider the transmitter to receiver path shown in Figure 14. For this path, the modeled signal

intersects 6 building outlines and 2 foliage boundaries. For this signal path, the distance is determined to be 142.8 meters. Using a path loss exponent of 2.8 and propagation effects for building outlines and foliage boundaries of 0.9dB and 0.4dB respectively, the total path loss given by the model under study at 2.412GHz is equal to 105.6dB. When the transmit power and antenna gain is included in the calculation, these parameter values for the model predict the RSSI for this location to be -79.0dBm (the actual measured RSSI was -79dBm).

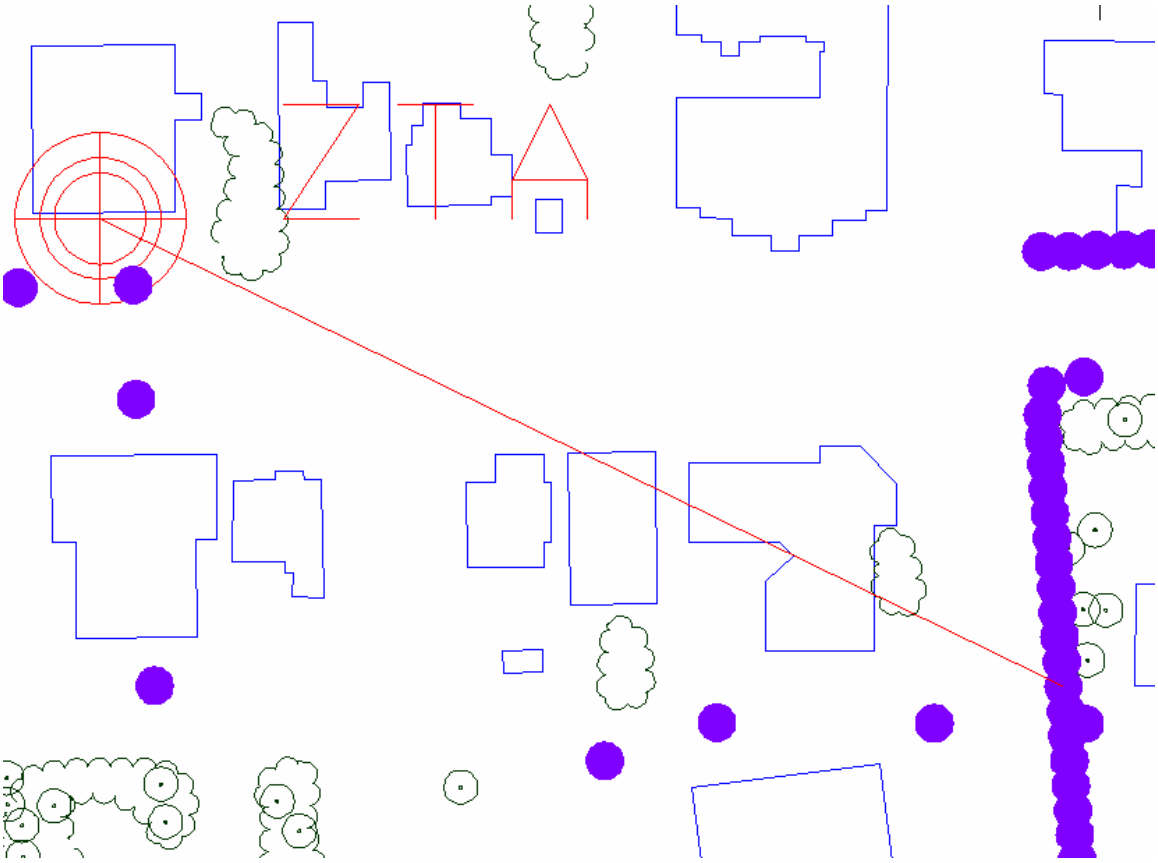

Figure 14: Diagram depicting a direct ray path from transmitter to receiver obtained from a screen-capture of the Motorola MeshPlanner™ software. The large circle in the upper left represents the ZTA AP, the small circles are measurement locations. The line from the AP to a measurement point is an example of the direct-ray used by the predictive model to determine the path loss from the transmitter to the receiver for that measurement location.

5.2: Parameter Values Obtained from Linear Regression

Figure 15 shows the locations of all measured points included in this analysis. As previously mentioned, each measurement location may contain measured values for more than one AP and therefore 523 total path loss measurements have been included in the analysis.

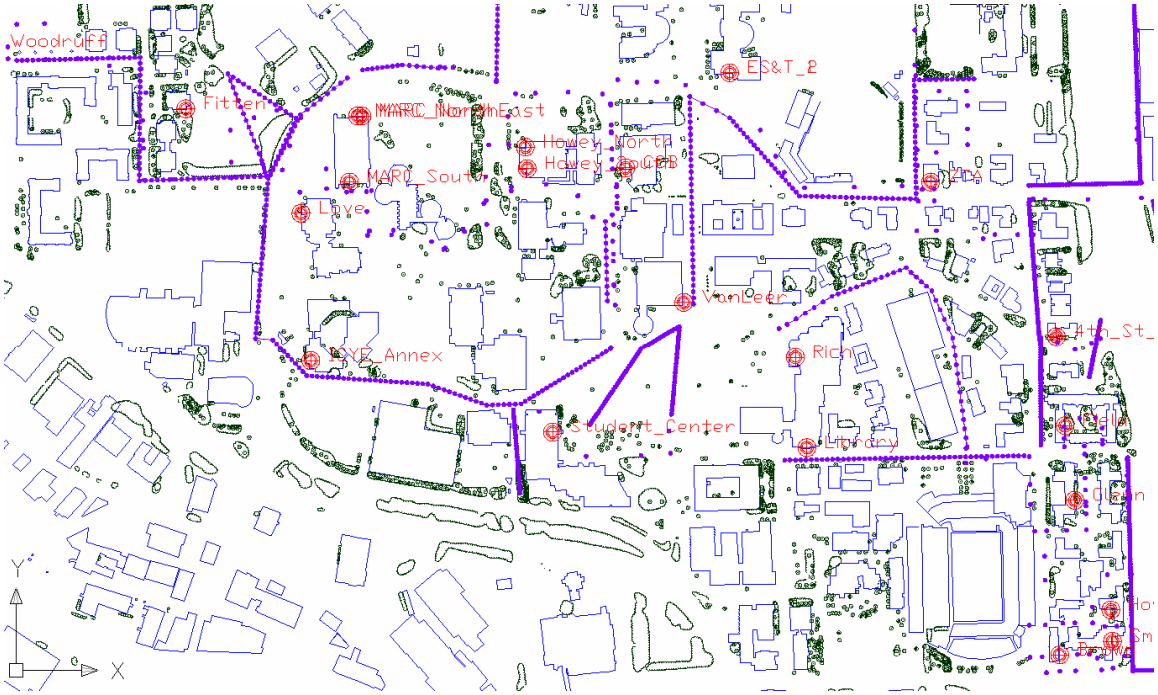

Figure 15: Diagram of measured portion of the campus of the Georgia Institute of Technology obtained from a screen-capture of the Motorola MeshPlanner™ software. Measurement locations are marked with a small, solid circle.

Table 1 provides the results of a regression analysis performed on the data taken on campus. Values for the model parameters are determined using a least-squares linear regression analysis [11], performed by the Optimatic functionality of Motorola MeshPlanner™. Also included are the calculated values for the model sensitivity to a given parameter ($\Delta\sigma$), which is calculated as the difference in the resulting standard deviation of the model error when that parameter is removed from the regression analysis

[11]. As seen in Table 1 the mean error is near zero and standard deviation of the model error is below 7dB for all samples of data, which indicates that the model can be used successfully in predicting AP deployment and planning.

Table 1: Model parameters obtained from a least-squares regression analysis of measurement data taken on the campus of the Georgia Institute of Technology.

AP Name, Lattitude, Longitude, Height	Path	# of pts	Path Loss Exponent		Building Footprint		Foliage Boundary		Mean error	std dev
			dB/ decade	Δσ	dB	Δσ	dB	Δσ		
Aggregate	All	523	2.65	23.4	0.5	0.2	0.6	0.3	0.3	6.6
	LOS	194	2.60						0.2	6.0
	NLOS	329	2.74	22.6	0.2	0.0	0.5	0.3	0.4	6.8
Van Leer 33.7757293 N 84.3968384 W 17.35 m	All	106	2.68	16.6	0.8	0.1	1.2	0.1	-0.1	6.6
	LOS	77	2.62						-0.1	6.3
	NLOS	29	3.11	27.8	-1.9	0.9	-0.1	0.0	0.1	4.8
TSRB South 33.7769982 N 84.3900884 W 22.27 m	All	204	2.56	26.8	0.2	0.0	0.6	0.3	0.2	5.1
	LOS	76	2.54						0.1	5.4
	NLOS	128	2.59	25.2	0.1	0.0	0.6	0.3	0.2	4.9
TSRB North 33.7774356 N 84.3899192 W 21.54 m	All	15	2.59	26.6	-1.8	2.8	-0.1	0.0	0.0	1.4
	LOS	4	2.57						0.1	1.4
	NLOS	11	2.61	23.0	-1.9	2.7	-0.2	0.1	0.0	1.3
ZTA 33.7770126 N 84.3932886 W 7.64 m	All	198	2.86	22.6	0.5	0.2	0.3	0.1	0.1	5.3
	LOS	37	2.76						0.2	5.6
	NLOS	161	2.95	20.9	0.2	0.0	0.3	0.1	0.0	5.0

In Table 1, negative values for propagation effect parameters may indicate some areas of the measurement environment in which there are propagation effects which more strongly correlate to signal gain with respect to free-space path loss, rather than signal loss with respect to free-space path loss. These areas are not considered to be significantly detrimental nor conclusive to the parameter values of the model however, since the number of data points for these regions is small in comparison to the data at large (e.g. for the TSRB North AP, there are only 15 total measurements for the AP) and

when the data is considered in total, the resulting parameters show stronger correlations to signal loss, which is more intuitively expected.

To illustrate, Figure 16 shows the correlation of transmitter to receiver distance, number of building wall intersections, and number of foliage boundary intersections to the measured RSSI for each direct-ray path according to the correlation coefficient of the sample sets. The correlation coefficient is calculated according to:

$$Correlation_{x,y} = \frac{\sum_{i}^{n}\left(\left(x_i - \bar{x}\right)\left(y_i - \bar{y}\right)\right)}{n \cdot \sigma_x \sigma_y} \qquad 6$$

where n is the total number of data points in a sample set, x_i and y_i are the values of an individual data point in two different sample sets, $\bar{x}$ and $\bar{y}$ are the mean values of the two different sample sets, and σ_x and σ_y are the standard deviations of the two different sample sets [13]. In Figure 16, a positive correlation occurs when the signal path loss increases as the test parameter increases. For example, path loss typically increases as transmitter to receiver distance increases, and as expected there is a relatively strong positive correlation between the signal path loss and the transmitter to receiver distance.

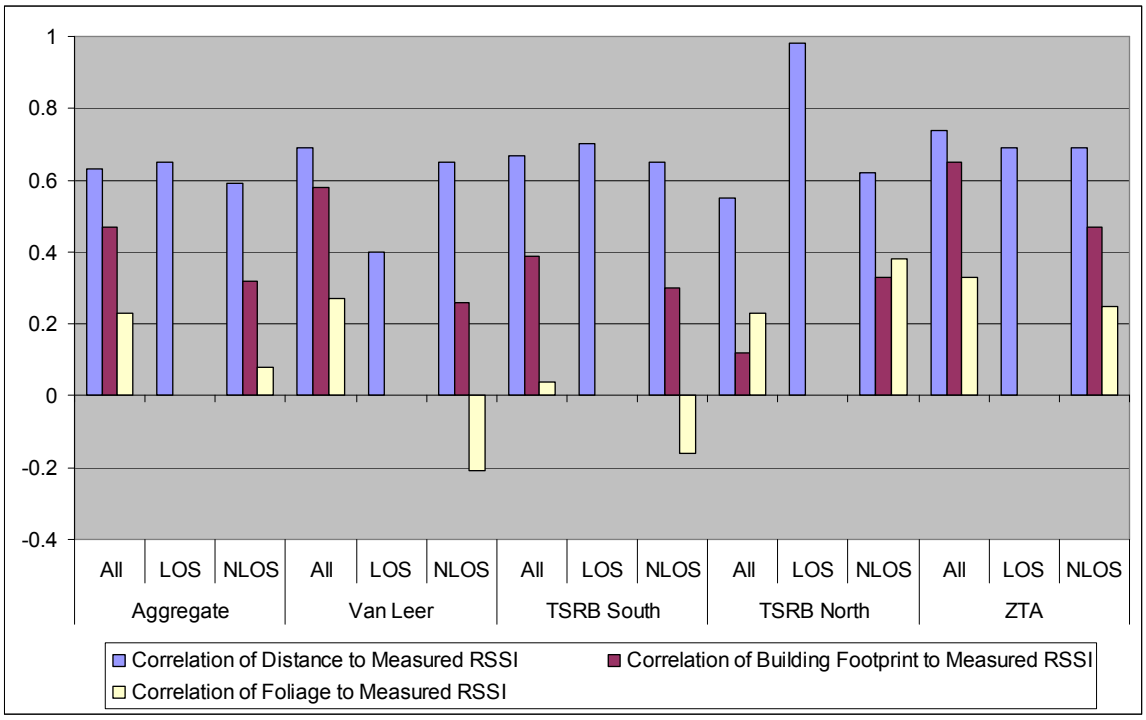

Figure 16: Chart showing the correlation of various model parameters to the actual measured RSSI for the transmitting AP.

As discussed previously, the footprints of known buildings and foliage boundaries for a large number of cataloged tree canopies in the area under study are included in the environment model. These were included so that the intersections between the modeled obstructions and the direct-ray path could be used both as independent model parameters, and also as a means of determining LOS and NLOS paths for comparison in the analysis. In the analysis it can be seen that for both the building outlines and the foliage boundaries, the obtained value for the building attenuation decreases when the analyzed data is reduced to only included NLOS paths for each data set.

It is likely that the optimal parameter values for the building and foliage propagation effects are reduced for the NLOS case due to a de-correlation of the model parameter to the overall path loss. For example, in the case when LOS and NLOS paths

are not differentiated in the analysis, the building and foliage propagation effects serve as the means for providing the necessary additional path loss to the model in NLOS paths, while still maintaining a lower path loss exponent which increases the model accuracy for LOS paths. When the LOS and NLOS paths are considered separately, the correlation of the building outlines and foliage boundaries to the measured RSSI decreases (for all sample sets except TSRB North and TSRB South foliage, where the lacking data for TSRB North has already been discussed and correlation of the foliage for the NLOS TSRB South paths may be attributed), and the path loss is determined more predominantly by the NLOS path loss exponent. Further, it is clear from the model sensitivity calculations that on the whole, the building and foliage propagation effects are largely used as correction factors in the propagation model. The path loss is dominated by the free space loss, and the building and foliage parameters function as added independent parameters to increase the overall model accuracy, but not largely affect the big-picture view of the path loss.

As it may seem from the discussion up to this point, the most important model parameters obtained from the analysis are the path loss exponents. These provide significant insight into the distance-dependent attenuation of the wireless signal, which is the largest path loss contributor in the model under study. In the analysis we can see that, as expected, the value for the path loss exponent is systematically higher for NLOS paths than it is for LOS paths. This indicates that, in general and as may be intuitively expected, the signal strength decreases faster for NLOS paths than it does for LOS paths. For the single path loss exponent model used in this study, this larger rate of path loss for

NLOS cases is accounted for by the inclusion of the building footprint and foliage boundary propagation effects.

5.3: Comparison to Published Values

In order to get a direct comparison of the performance of a propagation model with that of another, both models should be analyzed using the same set of data. As such analysis was performed for a single path loss exponent, purely distance dependent model given by the equation:

$$PathLoss = PL(d_0) + 10n\log_{10}\left(\frac{d}{d_0}\right) \quad (7)$$

where $PL(d_0)$ is equal to the free space path loss with respect to a given reference distance, d_0, d is the distance between the transmitter and receiver, and n is the path loss exponent. Table 2 shows the results of this model and the model under study.

Table 2: Comparison of Model Under Study (MUS) to single path loss exponent, purely distance dependent model (DDM). Results indicate the accuracy advantage of including site-specific building outline and foliage boundary data in the path loss model.

AP	# of Points	Path Loss Exponent		Mean error		Standard Deviation	
		MUS	DDM	MUS	DDM	MUS	DDM
Aggregate	523	2.65	2.75	0.3	0.2	6.6	7.1
Van Leer	106	2.68	2.72	-0.1	-0.2	6.6	6.8
TSRB South	204	2.56	2.61	0.2	0.2	5.1	5.4
TSRB North	15	2.59	2.42	0.0	0.3	1.4	4.2
ZTA	198	2.86	2.99	0.1	-0.1	5.3	5.6

As can be seen from Table 2, there is a clear accuracy benefit from including site-specific building outline and foliage boundary data in the path loss model. On average the model under study (labeled as MUS), had a 0.8dB decrease in prediction error as compared to the distance dependent model (labeled as DDM).

When performing analysis on any model, it is also important to compare the results with the existing results of other's research. Therefore, some of the parameters obtained from analysis of the model under study are here compared with those of other models at similar frequencies and environments.

Since most other models have not used building outlines and foliage boundaries in the same manner as the model under study, there is little-to-no direct comparison that can be made for those parameters as obtained from the previously discussed analysis results. The obtained path loss exponents, however, are frequently used in most all models, and as such, Table 3 is provided which contains published values for other models in similar environments and the previously discussed distance dependent model. As can be seen, the path loss exponents of the model under study are in agreement with those of the other models. There are some differences between models both at this frequency range and at others, but this can be expected since the inclusion of various additional parameters and differing methods of determining model parameters will affect the obtained path loss exponent value.

Table 3: Comparison of the path loss exponent values obtained for the model under study to a single path loss exponent, purely distance dependent model and several published path loss models.

Model	Frequency [GHz]	Type	Path Loss Exponent [dB/decade]
Model Under Study	2.4	Direct Ray	2.5 - 3.7
Distance Dependent Model	2.4	Direct Ray	2.4 - 3.0
Xia et al 94 [7]	1.9	Direct Ray	2.5 - 5.0
Piazzi & Bertoni 99 [10]	1.8	Multi Ray	3.9 - 5.9

Table 4 shows the standard deviation of the model error for various published models, as well as the results of the single path loss exponent, purely distance dependent

model. From the data it is clear that the model under study performs comparably well in terms of accuracy for the area under analysis. As stated previously, an improved comparison would analyze each model for the same environment and the same measurements as performed for the purely distance dependent model, but this is not included in the scope of the current study; perhaps future research will allow these analyses.

Table 4: Comparison of the standard deviation of the model error for the model under study to a single path loss exponent, purely distance dependent model and several published path loss models.

Model	Frequency [GHz]	Type	Standard Deviation [dB]
Model Under Study	2.4	Direct Ray	5.0 - 6.5
Distance Dependent Model	2.4	Direct Ray	5.5 - 7.0
Xia et al '94 [7]	1.9	Direct Ray	5.0 - 9.0
Aschrafi et al '06 [8]	2.1	Multi Ray	6.7
Erceg et al '97 [9]	2	Multi Ray	4.4
Piazzi & Bertoni '99 [10]	1.8	Multi Ray	4.7

CHAPTER 6:
PREDICTIONS BASED ON NEW MODEL PARAMETERS

As discussed previously, the Adaptive Deployment method of outdoor WLAN network development promises lowered cost and lowered time-to-deployment. By performing the placement, measurement, and analysis processes on an initial test area and then use the analysis of this test area to update parameters for a predictive model, the model can then be used to simulate the deployment process in other areas. Therefore, as a test to further verify the validity of the model used in this analysis and examine the validity of the Adaptive Deployment philosophy, predictions were made at measured locations not included in the model regression analysis. Specifically, the aggregate regression results were used to predict the RSSI for the measurement points of each area individually, and also the regression results for each individual area were used to predict the RSSI for the measurement points of the other areas. The resulting mean error, $\bar{e}$, and standard deviation, σ, in dB for each of these predictions is given in Table 5.

Table 5: Results for predictions of the model under study at measured locations not included in the regression analysis used to obtain the model parameters.

		Prediction Area									
Source Area	# of pts	Aggregate		Van Leer		TSRB South		TSRB North		ZTA	
		$\bar{e}$	σ	$\bar{e}$	σ	$\bar{e}$	σ	$\bar{e}$	σ	$\bar{e}$	σ
Aggregate	523			0.7	6.7	-3.0	5.4	-6.5	5.8	4.1	5.3
Van Leer	106	-1.8	7.0			-5.3	5.9	-8.2	1.4	1.3	6.2
TSRB South	204	3.3	6.6	2.9	6.8			0.2	5.1	7.4	5.5
TSRB North	15	8.9	10.3	3.6	7.8	5.8	8.8			15.6	9.6
ZTA	198	-4.0	6.9	-3.5	6.6	-7.9	5.7	-11.1	6.3		

In Table 5, the model parameter values used for each prediction are derived using values from measurements not included in the prediction area; with the exception of predictions into all areas (aggregate). The results show that the predictions maintain a satisfactorily tight fit with the average standard deviation being 6.5dB. However, the results nearly all show significant offsets in the mean error, which agrees with the results found for a similar analysis by Piazzi and Bertoni using various modeling methods [10].

The fact that the standard deviation remains relatively low when predicting into new areas agrees with the previous analysis in Chapter 5, which indicated that the path loss was most significantly due to the free space path loss, and that the building outline and foliage boundary information had less significant effects. Perhaps highlighting the relatively small effects of the building outline and foliage boundary information however, predictions made using the same methodology as above, but using the purely distance dependent model yielded similar results as shown in Table 6. In fact, on average there is very little difference between the results obtained for the two models.

This result shows that the inclusion of site-specific building outlines and foliage boundaries does not decrease the average prediction accuracy into new environments as compared with the purely distance dependent model. In fact, it appears that the inclusion of the additional parameters provides an increase in accuracy in some predictions, and the decrease in accuracy found in others may be attributed to a low measurement count.

Table 6: Results for predictions of the single path loss exponent, purely distance dependent model at measured locations not included in the regression analysis used to obtain the model parameters.

Source Area	# of pts	Prediction Area									
		Aggregate		Van Leer		TSRB South		TSRB North		ZTA	
		$\bar{e}$	σ	$\bar{e}$	σ	$\bar{e}$	σ	$\bar{e}$	σ	$\bar{e}$	σ
Aggregate	523			-1.0	6.8	-3.5	5.6	-7.5	4.9	5.0	5.7
Van Leer	106	1.1	7.1			-2.6	5.5	-6.6	4.8	5.8	5.7
TSRB South	204	3.6	7.0	2.1	6.9			-4.1	4.6	8.2	5.8
TSRB North	15	7.9	7.0	6.0	7.1	4.9	5.3			12.3	6.0
ZTA	198	-5.1	7.3	-5.8	6.7	-9.3	5.8	-12.9	5.3		

This mean offset when predicting into new environments does not necessarily prohibit the Adaptive Deployment method for designing outdoor WLAN deployments. When the mean error offsets incurred from predictions into all data points (Aggregate), using optimal parameter values obtained from a subset of data (Van Leer, TSRB South, TSRB North, ZTA), are analyzed with respect to how many data points were used to obtain the original optimal parameters it is clear that the offset is worst in the situation where the measurement data is limited, TSRB North. If this TSRB North AP data is not considered, then the average mean error offset for predictions at all data points is only -0.9dB, which is considerably less troublesome. This suggests that the quality of the measurement survey used for the determination of the initial parameter set can have significant effects on the accuracy of predictions made into new environments.

CHAPTER 7:
CONCLUSIONS

7.1: Performance of the Model Under Study

From the analysis performed on measurements taken at the campus of the Georgia Institute of Technology, we can see that a simplistic direct-ray, single path loss exponent, adaptation of the Seidel-Rappaport model can yield satisfactory results in terms of model accuracy for outdoor microcell environments. Obtained path loss values agree with those previously published in other research, and the standard deviation of the model error is similar to that of other models. Additionally, these results confirm the validity of using a standard, consumer WLAN card for measurement surveys intended for model analysis.

Further, this direct-ray model appears to strike the perfect balance between simplicity and accuracy. It is significantly more accurate than purely distance dependent methods, while requiring only modest amounts of additional site information. Additionally, what gains in accuracy that may possibly be obtained by using a more complicated multi-ray model, are detrimentally offset by the added requirement of highly accurate site-specific information and vastly increased computation time. This lends credence to the possibility of using simpler, less sophisticated models to perform pre-deployment predictive planning of wireless networks.

7.2: Viability of the Adaptive Deployment Design Methodology

The Adaptive Deployment network design methodology was also verified as being an effective, accurate method for planning network infrastructure development. By performing initial site-survey and analysis on test areas in order to develop general model

parameters for deployment simulation, this development methodology can drastically reduce the amount of time required to deploy a WLAN network, and therefore also reduce the cost associated with deployment. Using the Adaptive Deployment method combined with the direct-ray, single path loss exponent, Seidel-Rappaport outdoor path loss model, there is potential faster deployment of WLAN networks at lower cost and better quality of service.

BIBLIOGRAPHY

[1] T.K. Sarkar, Z. Ji, K. Kim, A. Medouri, and M. Salazar-Palma, "A Survey of Various Propagation Models for Mobile Communications," *IEEE Antennas and Propagation Magazine*, Vol. 45, No. 3, June 2003, pp. 51 – 82.

[2] T.S. Rappaport and L.B. Milstein, "Effect of Radio Propagation Path Loss on DS-CDMA Cellular Frequency Reuse Efficiency for the Reverse Channel," *IEEE Transaction on Vehicular Technology*, VT-48, 5, August 1999, pp. 1451 – 1452.

[3] H. Xia, H.L. Bertoni, L.R. Maciel, A. Lindsay-Stewart, and R. Rowe, "Radio Propagation Characteristics for Line-of-Sight Microcellular and Personal Communications," *IEEE Transactions on Antennas and Propagation*, AP-41, 10, October 1993, pp. 1439 – 1447.

[4] M.J. Feuerstein, K.L. Blackard, T.S. Rappaport, S.Y. Seidel, and H.H. Xia, "Path Loss, Delay Spread, and Outage Models as Functions of Antenna Height for Macrocellular System Design," *IEEE Transactions on Vehicular Technology*, VT-43, 3, August 1994, pp. 487 – 498.

[5] S. Y. Seidel, and T. S. Rappaport, "914 MHz Path Loss Prediction Models for Indoor Wireless Communications in Multifloored Buildings," IEEE Transactions on Antennas and Propagation, vol. 40, no. 2, February 1992, pp. 207 – 217.

[6] J. B. Anderson, T.S. Rappaport, and S. Yoshida, "Propagation Measurements and Models for Wireless Communications Channels," *IEEE Communications Magazine*, January 1995, pp. 42 – 49.

[7] H. Xia, H. Bertoni, L. Maciel, A. Lindsay-Stewart, and R. Rowe, "Microcellular Propagation Characteristics for Personal Communications in Urban and Suburban Environments," *IEEE Transactions on Vehicular Technology*, vol. 43, no. 3, August 1994, pp. 743 – 752.

[8] Aschrafi, P. Wertz, M. Layh, F.M. Landstorfer, G. Wölfe, and R. Wahl, "Impact of Building Database Accuracy on Predictions with Wave Propagation Models in Urban Scenarios," *IEEE Vehicular Technology Conference*, vol. 6, 2006, pp. 2681-2685.

[9] V. Erceg, S. J. Fortune, J. Ling, A. J. Rustako, Jr., R. A. Valenzuela, "Comparisons of a Computer-Based Propagation Prediction Tool with Experimental Data Collected in Urban Microcellular Environments," *IEEE Journal on Selected Areas in Communications*, vol. 15, no. 4, May 1997, pp. 677 – 684.

[10] L. Piazzi, and H. Bertoni, "Achievable Accuracy of Site-Specific Path-Loss Predictions in Residential Environments," *IEEE Transactions on Vehicular Technology*, vol. 48, no. 3, May 1999, pp. 922 – 930.

[11] G.D. Durgin, T. S. Rappaport, and H. Xu, "Measurements and Models for Radio Path Loss and Penetration Loss In and Around Homes and Trees at 5.85 GHz," *IEEE Transactions on Communications*, vol. 46, no. 11, November 1998, pp. 1484 – 1496.

[12] R. R. Skidmore, "A Comprehensive In-Building and Microcellular Wireless Communication System Design Tool," M.S. thesis, Dept. Elect. Eng., Virginia Polytechnic Inst. and State Univ., Blacksburg, VA, 1997.

[13] Weisstein, Eric W. "Correlation Coefficient." From *MathWorld*--A Wolfram Web Resource. http://mathworld.wolfram.com/CorrelationCoefficient.html

[14] M. F. Iskander, and Z. Yun, "Propagation Prediction Models for Wireless Communication Systems," *IEEE Transactions on Microwave Theory and Techniques*, vol. 50, no. 3, March 2002, pp. 662 – 673.

[15] A. J. Rustako, N. Amitay, G. J. Owens, and R. R. Roman, "Radio Propagation at microwave frequencies for line-of-sight microcellular mobile and personal communications," *IEEE Transactions on Vehicular Technology*, vol. 40, Feb. 1991, pp. 203 – 210.

[16] G. Wölfle, and F. M. Landstorfer, "Dominant Paths for the Field Strength Prediction," *IEEE Vehicular Technology Conference*, vol. 1, May 1998, pp. 552 – 556.

[17] S. R. Saunders, and F. R. Bonar, "Prediction of Mobile Radio Wave Propagation Over Buildings of Irregular Heights and Spacings," *IEEE Transactions on Antennas and Propagation*, vol. 42, no. 2, Feb. 1994, pp. 137 – 144.

[18] J. Walfisch, and H. L. Bertoni, "A Theoretical Model of UHF Propagation in Urban Environments," *IEEE Transactions on Antennas and Propagation*, vol. 36, no. 12, Dec. 1988, pp. 1788 – 1796.

[19] K. Low, "Comparisons of Urban Propagation Models with CW-Measurements," *IEEE Vehicular Technology Society 42nd VTS Conference*, vol. 2, May 1992, pp. 936 – 942.